Chapter IV

CHAPTER IV

SIMPLE SALTS OF NAPHTHOIC ACIDS WITH AMINOGUANIDINE /GUANIDINE: PREPARATION AND THEIR THERMAL CHARACTERIZATION

4.1. INTRODUCTION

Aminoguanidine (AMG) is a hydrazine derivative of bifunctional group, it is expected that the salts made from aminoguanidine will be similar to the hydrazine moiety. The increased thermal and chemical reactivity of aminoguanidine is due to its nitrogen component and asymmetric bifunctional structure. In the solid state, aminoguanidine occurs as a mono (+1) or di (+2) cation, but it is unstable in the free state. In addition non-hydrogen atoms remain in the sp^2 hybridized state, and the extreme nitrogen atom takes part in the sp^3 hybridized state in the solid form [123].

Guanidine (GUA) is an organic compound with the formula $HNC(NH_2)_2$. It is present as guanidinium ion and it is the strongest organic base. It contains at least one CN_3 moiety with a dissociation behavior of π- electrons. The high basicity of guanidines is due to the resonance stabilization of delocalized π- electrons in CN_3 moiety [4].

Naphthoic acid is an organic molecules having a double-fused benzene rings and have a functional group of -COOH. Hydroxy naphthoic acid shows a very good bidentate ligand and coordinates by carboxylate and hydroxyl oxygen [5]. The study of the interaction between aminoguanidine, and guanidine with 1-naphthoic acid, and 2-naphthoic acid, and their IR and thermal characterization are presented in this chapter.

4.2 PREPARATION OF SALTS

The salts were prepared by mixing the solutions of respective acid and base in 40 mL of water-alcohol mixture at appropriate ratios (1:1, 1:2, and 2:1), as shown in **Table 4.1**.

Table 4.1 *Preparation of aminoguanidinium and guanidinium salts.*

Acid: Base	Molar ratio (acid: base)	pH	Chemical composition
1-naphthoic acid: aminoguanidine (0.172g:0.136g)	1:1	7	$[(CH_5N_4)\{(C_{10}H_7)(1\text{-}COO)\}]$
1-naphthoic acid: aminoguanidine (0.172g:0.272g)	1:2	8	$[(CH_5N_4)_2\{(C_{10}H_7)(1\text{-}COO)\}]$
1-naphthoic acid: aminoguanidine (0.344g:0.136g)	2:1	7	$[(CH_5N_4)\{(C_{10}H_7)(1\text{-}COO)\}_2]$
1-naphthoic acid: guanidine (0.172g:0.090g)	1:1	7	$[(CH_4N_3)\{(C_{10}H_7)(1\text{-}COO)\}]$
1-naphthoic acid: guanidine (0.172g:0.180 g)	1:2	8	$[(CH_4N_3)_2\{(C_{10}H_7)(1\text{-}COO)\}]$
1-naphthoic acid: Guanidine (0.344g:0.090g)	2:1	7	$[(CH_4N_3)\{(C_{10}H_7)(1\text{-}COO)\}_2]$
2-naphthoic acid: aminoguanidine (0.172g:0.136g)	1:1	7	$[(CH_5N_4)\{(C_{10}H_7)(2\text{-}COO)\}]$
2-naphthoic acid: aminoguanidine(0.172g:0.272g)	1:2	8	$[(CH_5N_4)_2\{(C_{10}H_7)(2\text{-}COO)\}]$
2-naphthoic acid: aminoguanidine(0.344g:0.136g)	2:1	7	$[(CH_5N_4)\{(C_{10}H_7)(2\text{-}COO)\}_2]$
2-naphthoic acid: guanidine (0.172g:0.180 g)	1:2	8	$[(CH_4N_3)_2\{(C_{10}H_7)(2\text{-}COO)\}]$
2-naphthoic acid: guanidine (0.344g:0.090g)	2:1	7	$[(CH_4N_3)\{(C_{10}H_7)(2\text{-}COO)\}_2]$

By preparing the above salts by test method crystalline adduct were found to form in the molar ratios which are indicated in **Table 4.2.**

Table 4.2 *Preparation of guanidinium salt with 2-naphthoic acid.*

Acid: Base	Molar ratio	pH	Chemical composition
2-naphthoic acid: Guanidine (0.172g:0.090g)	1:1	7	$[(CH_4N_3)\ \{(C_{10}H_7)(2\text{-}COO)\}]$

A homogenous clear solution thus obtained was kept undisturbed for 15 days at room temperature. A product found as shiny colourless crystals obtained from the mother liquid it was drained, and washed with alcohol, diethyl ether, then kept in anhydrous calcium chloride in a desiccator for dried. The crystal structure and its related characterization were discussed in Chapter 5.

4.3 RESULT AND DISCUSSION

4.3.1 Analytical Data

The analytical data for the proposed salts with molecular formulae which was illustrated in **Table 4.3**.

4.3.2 FT-IR spectral data

In **Table 4.3,** the important IR band for the salts is listed, and **Figures 4.1(a-f)-4.2(a-f)** represent the IR spectra of corresponding salts.

The spectral data of all aminoguanidium/ guanidium naphthoate exhibit broadband around 3034-3321 cm^{-1} due to the presence of a -OH molecule. The presence of N-N frequency was confirmed by the presence of a peak around 1098-1381 cm^{-1}. The carboxylate ions region around 1350-1430 cm^{-1} and 1501-1572 cm^{-1}. The absorption peak occur from 1085-1381 cm^{-1} is due to N-N stretching frequency of aminoguanidine for guanidine it occurs at 648-776 cm^{-1}. The presence of peaks at 3034-3321, 1018-1068, 1475-1518, and 1098-1351 cm^{-1} is evidence for the formation of salts where these peaks are absent in the IR spectra of pure acid [62].

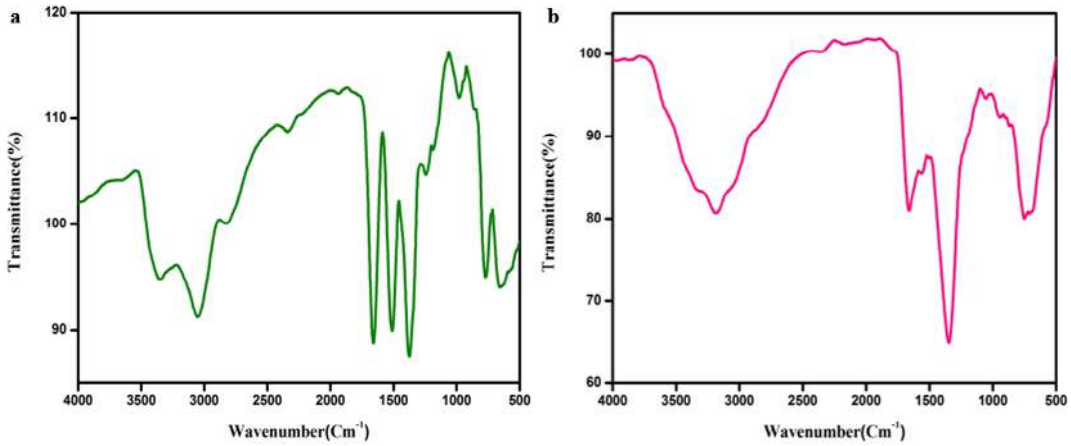

Figures 4.1 *FT-IR spectra of a) [(CH5N4){(C10H7)(1-COO)}] b) [(CH5N4)2{(C10H7)(1-COO)}]*

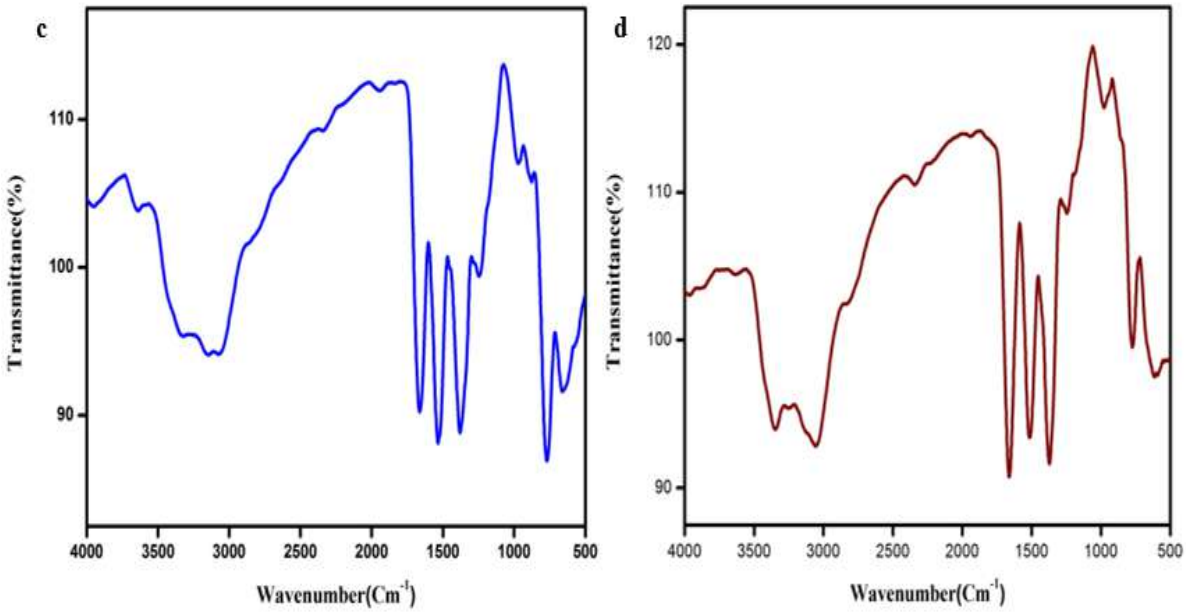

Figures 4.1 *FT-IR spectra of c) [(CH5N4){(C10H7)(1-COO)}2] d) [(CH4N3){(C10H7)(1-COO)}]*

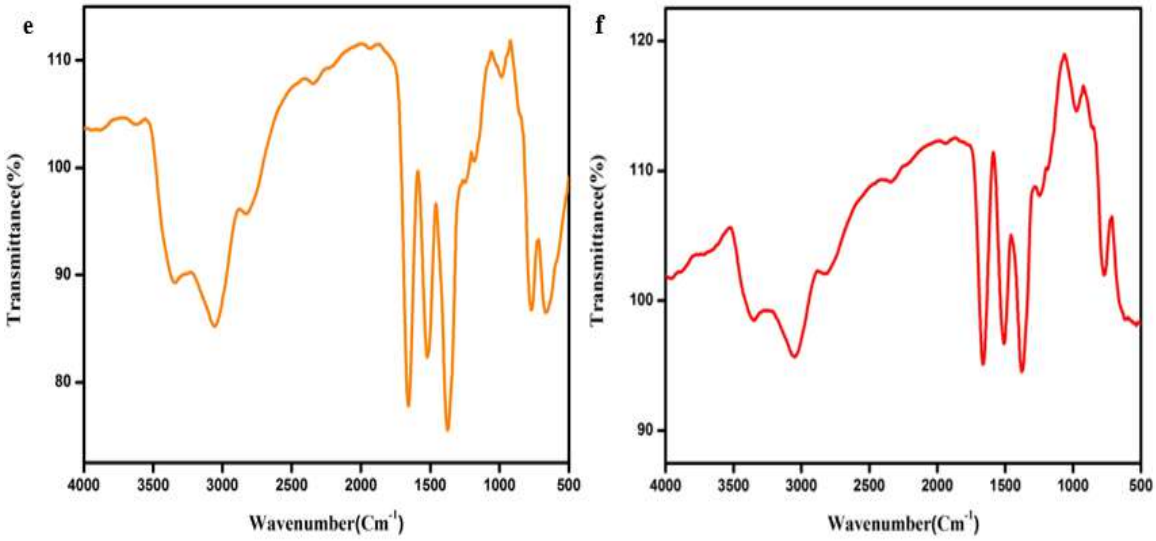

Figures 4.1 *FT-IR spectra of e) $[(CH_4N_3)_2\{(C_{10}H_7)(1\text{-}COO)\}]$ f) $[(CH_4N_3)\{(C_{10}H_7)(1\text{-}COO)\}_2]$*

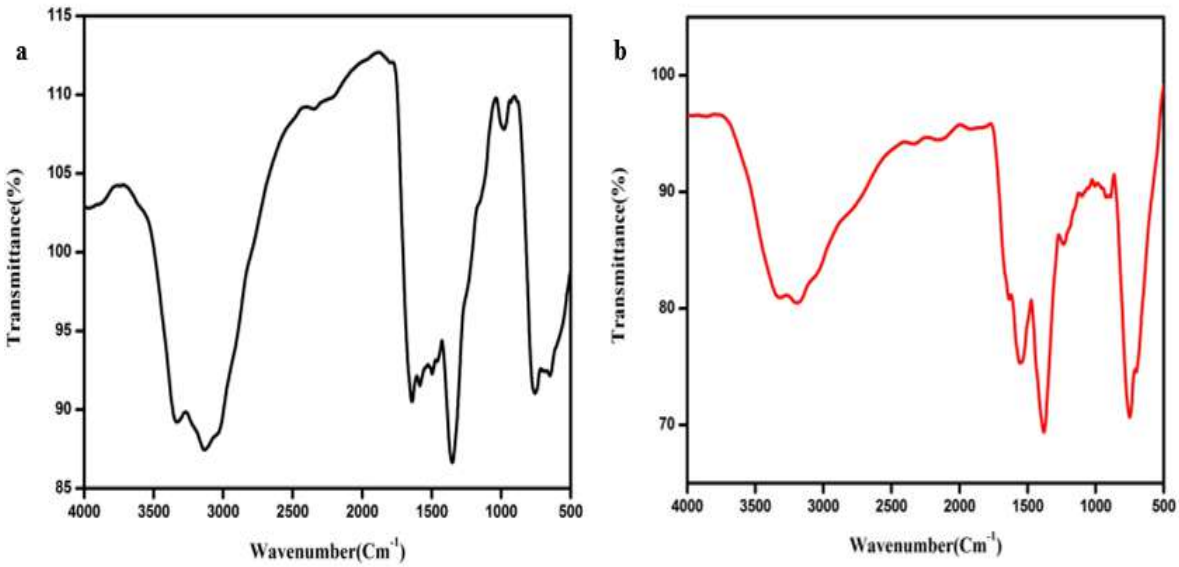

Figures 4.2 *FT-IR spectra of a) $[(CH_5N_4)\{(C_{10}H_7)(2\text{-}COO)\}]$ b) $[(CH_5N_4)_2\{(C_{10}H_7)(2\text{-}COO)\}]$*

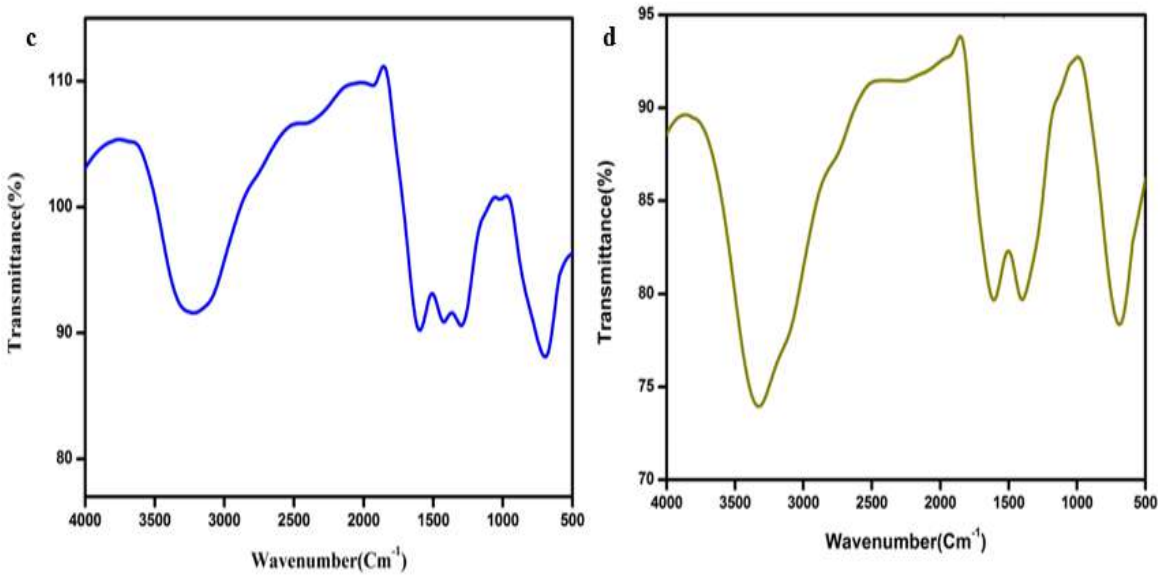

Figures 4.2 *FT-IR spectra of c) [(CH5N4){(C10H7)(2-COO)}2] d) [(CH4N3){(C10H7)(2-COO)}]*

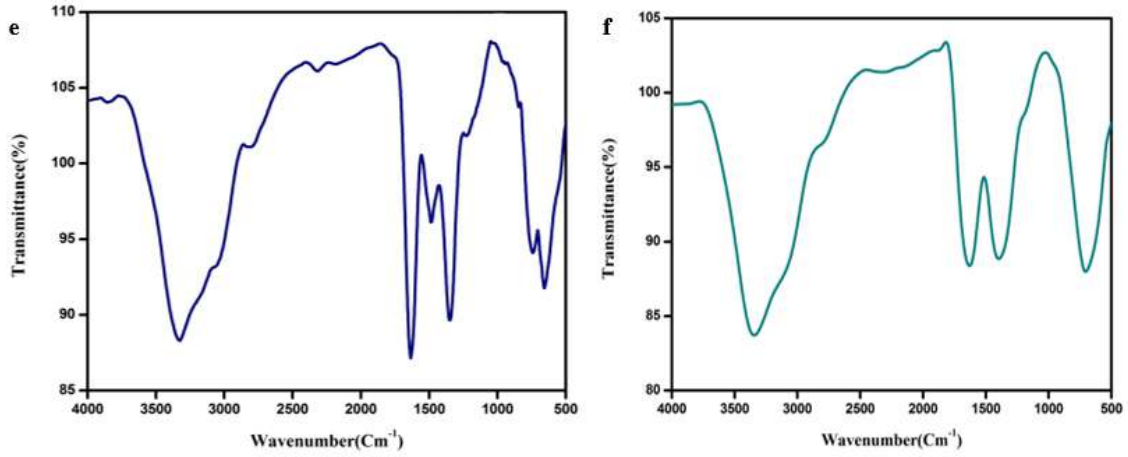

Figures 4.2 *FT-IR spectra of e) [(CH4N3)2{(C10H7)(2-COO)}] f) [(CH4N3){(C10H7)(2-COO)}2]*

Table 4.3 *Element Analysis and IR Spectra.*											
Ligand	**Molecular Weight**	**Melting point °C**	**Analytics data**				**IR data**				
			Carbon (Fd) (calcd.)	**Hydrogen (Fd) (calcd.)**	**Nitrogen (Fd) (calcd.)**	**Hydrazine (Fd) (calcd.)**	$\nu_{(OH)}$ cm^{-1}	ν_{asym} (C=O) cm^{-1}	υ_{sym} (C=O) cm^{-1}	$\upsilon_{(NH)}$ cm^{-1}	$\upsilon_{(N-N)}$ cm^{-1}
$[(CH_5N_4)\{(C_{10}H_7)(1\text{-}COO)\}]$	244.10	162	59.01 (59.00)	4.95 (4.94)	22.94 (22.95)	12.6 (12.7)	3034	1668	1529	3372	1098
$[(CH_5N_4)_2\{(C_{10}H_7)(1\text{-}COO)\}]$	318.16	150	49.05 (49.04)	5.70 (5.69)	35.20 (35.19)	7.9 (7.10)	3175	1670	1540	3343	1085
$[(CH_5N_4)\{(C_{10}H_7)(1\text{-}COO)\}_2]$	414.13	117	66.66 (66.65)	4.38 (4.36)	13.52 (13.51)	14.9 (14.10)	3114	1668	1519	3659	1212
$[(CH_4N_3)\{(C_{10}H_7)(1\text{-}COO)\}]$	229.03	121	62.87 (62.86)	4.84 (4.83)	18.33 (18.32)	11.2 (11.3)	3046	1650	1511	3363	776
$[(CH_4N_3)_2\{(C_{10}H_7)(1\text{-}COO)\}]$	288.31	110	54.16 (54.15)	5.59 (5.58)	29.15 (29.10)	10.9 (10.10)	3074	1669	1519	3322	648
$[(CH_4N_3)\{(C_{10}H_7)(1\text{-}COO)\}_2]$	399.40	160	69.17 (69.15)	4.29 (4.28)	10.52 (10.51)	12.5 (12.6)	3036	1659	1511	3344	767
$[(CH_5N_4)\{(C_{10}H_7)(2\text{-}COO)\}]$	244.25	152	59.01 (59.00)	4.95 (4.94)	22.94 (22.93)	11.6 (11.5)	3134	1649	1510	3352	1331
$[(CH_5N_4)_2\{(C_{10}H_7)(2\text{-}COO)\}]$	318.36	159	49.05 (49.03)	5.70 (5.69)	35.20 (35.19)	11.2 (11.3)	3193	1618	1559	3372	1381
$[(CH_5N_4)\{(C_{10}H_7)(2\text{-}COO)\}_2]$	414.41	162	66.6 (66.5)	4.38 (4.36)	13.52 (13.51)	10.5 (10.4)	3242	1638	1529	3421	1351
$[(CH_4N_3)_2\{(C_{10}H_7)(2\text{-}COO)\}]$	288.31	159	54.16 (54.15)	5.59 (5.50)	29.15 (29.14)	12.5 (12.6)	3322	1638	1480	3876	628
$[(CH_4N_3)\{(C_{10}H_7)(2\text{-}COO)\}_2]$	286.29	112	54.54 (54.53)	4.93 (4.92)	29.35 (29.30)	12.6 (12.7)	3321	1622	1475	3855	668

4.3.3 Uv-visible spectra and band gap energy

The spectral data for the ligand were recorded in the visible region from 200-800 nm at room temperature and it was illustrated in **Figure 4.3(a-l)**. All the ligand shows a band around at 250-350 nm, which resembles to $\pi \rightarrow \pi^*$, which is consistent with the naphthalene ring. The aminoguanidine base group undergoes $n \rightarrow \pi^*$ transition with a prominent absorption band around the 356-420 nm range.

The band gap energy was determined from UV-spectra using Tauc's plot, which was illustrated in **Figure 4.4(a-l)** by the resulting equation **Eq. (4.1)**.

$$(\alpha h\upsilon) = A(h\upsilon - E_g)^n \qquad \textbf{Eq. (4.1)}$$

where α = absorption coefficient, A = constant, h = planks constant, v = frequency of the photon, and E_g= optical bandgap. The calculated bandgap energy for all the ligand the ranges occur from 2.5-3.5 eV [7].

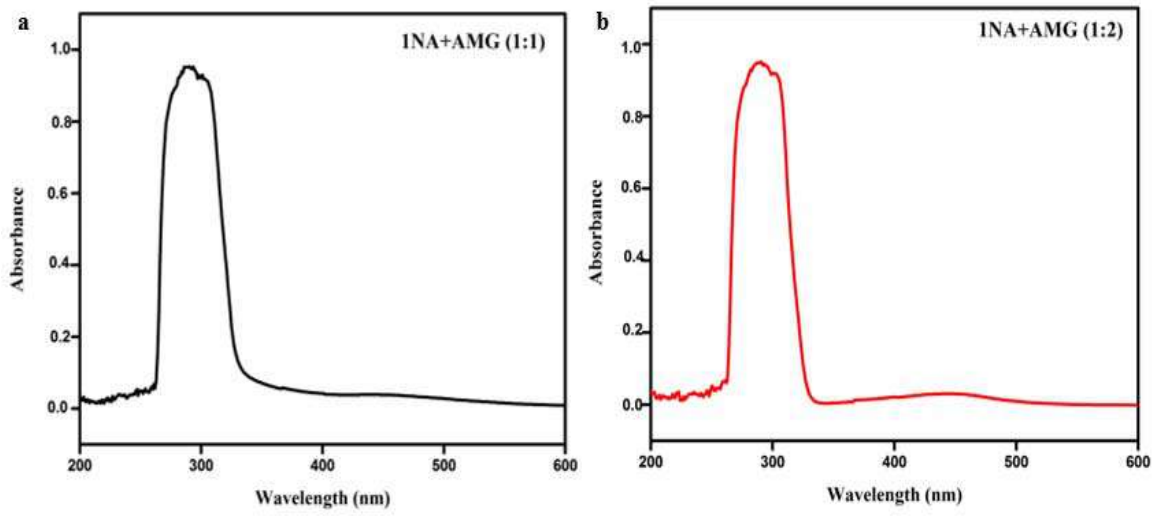

Figure 4.3 *UV-visible Spectra of a) [(CH_5N_4){($C_{10}H_7$)(1-COO)}] b) [(CH_5N_4)$_2${($C_{10}H_7$)(1-COO)}]*

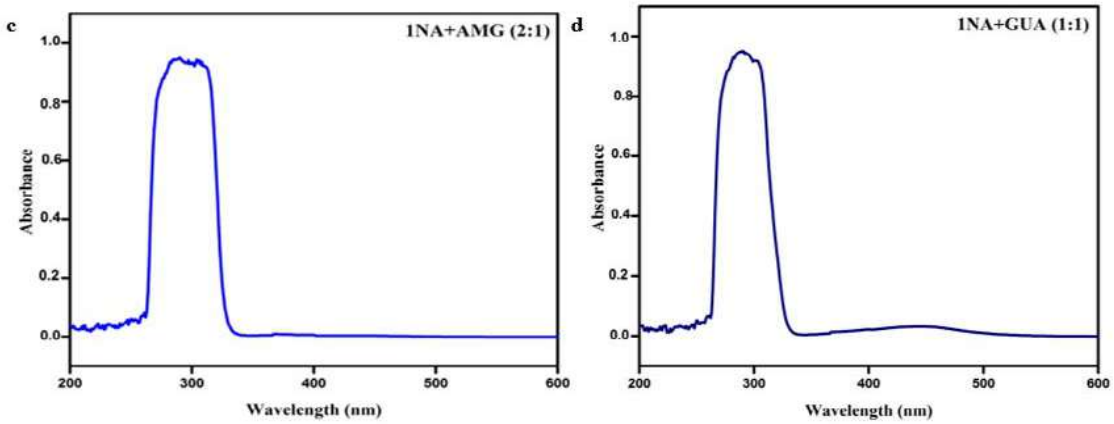

Figure 4.3 *UV-visible Spectra of c) [(CH5N4){(C10H7)(1-COO)}2] d) [(CH4N3){(C10H7)(1-COO)}]*

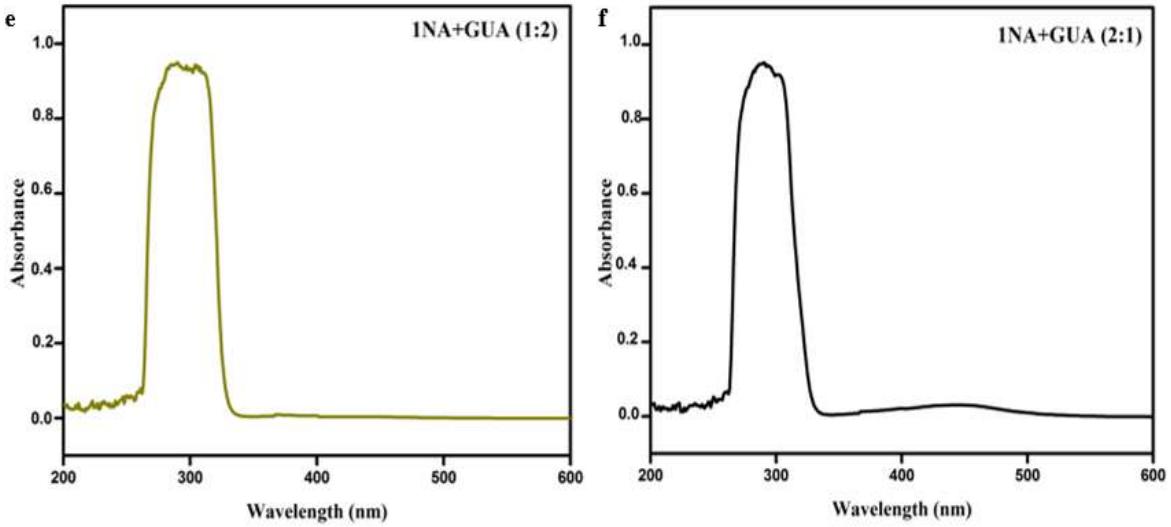

Figure 4.3 *UV-visible Spectra of e) [(CH4N3)2{(C10H7)(1-COO)}] f) [(CH4N3){(C10H7)(1-COO)}2]*

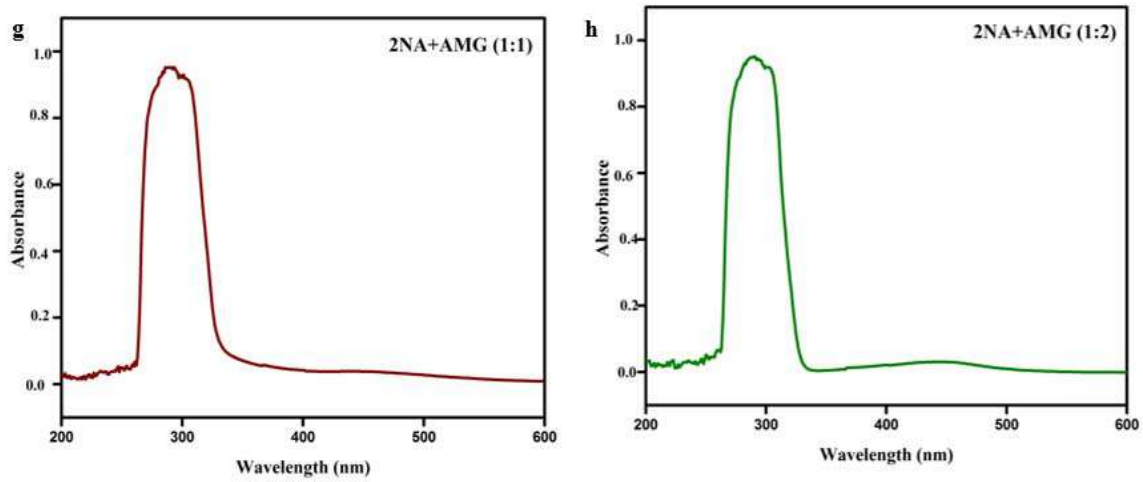

Figure 4.3 *UV-visible Spectra of g) [(CH_5N_4){($C_{10}H_7$)(2-COO)}] h) [(CH_5N_4)$_2${($C_{10}H_7$)(2-COO)}]*

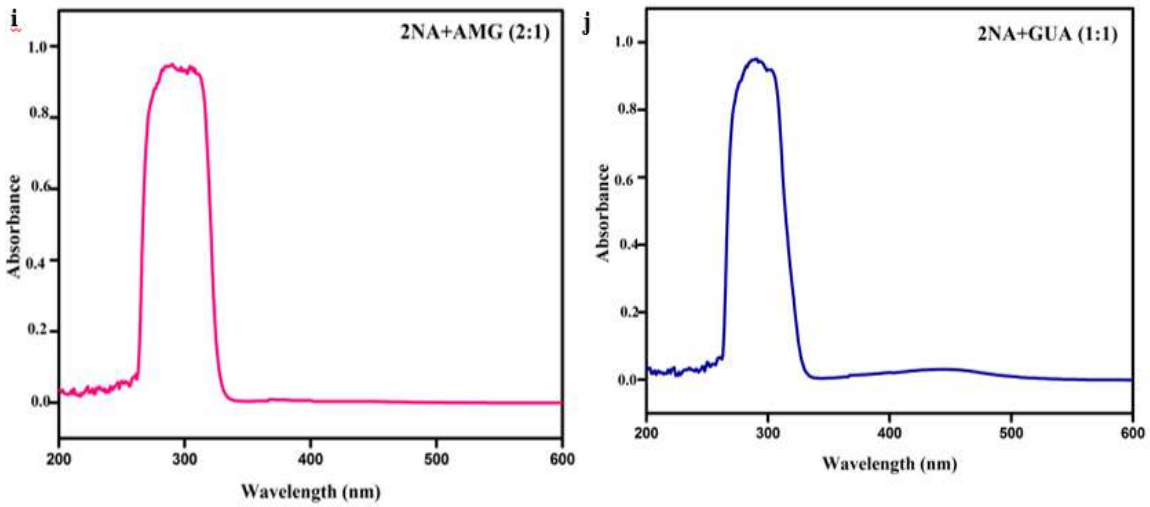

Figure 4.3 *UV-visible Spectra of i) [(CH_5N_4){($C_{10}H_7$)(2-COO)}$_2$] j) [(CH_4N_3){($C_{10}H_7$)(2-COO)}]*

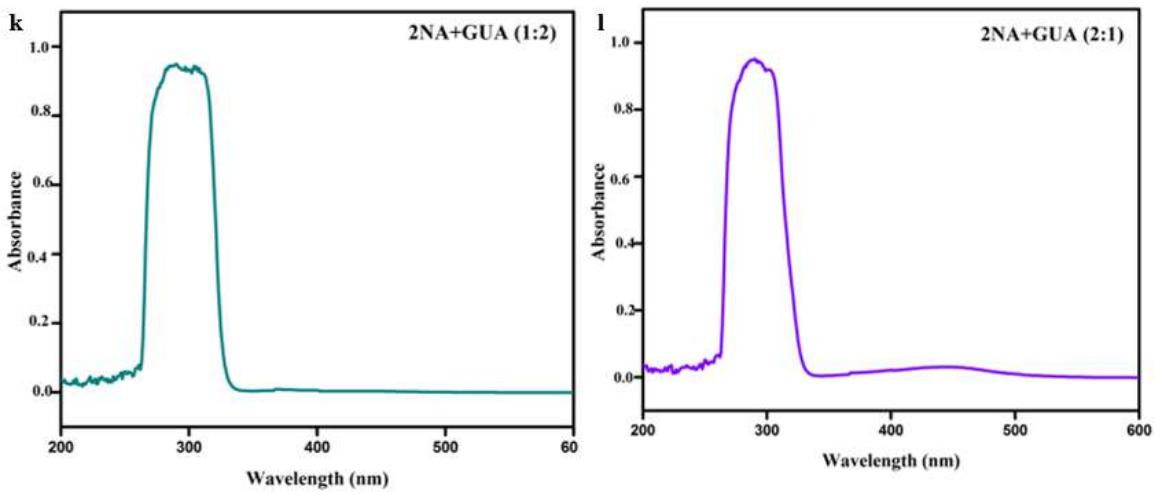

Figure 4.3 *UV-visible Spectra of k) [$(CH_4N_3)_2\{(C_{10}H_7)(2\text{-}COO)\}$]l) [$(CH_4N_3)\{(C_{10}H_7)(2\text{-}COO)\}_2$]*

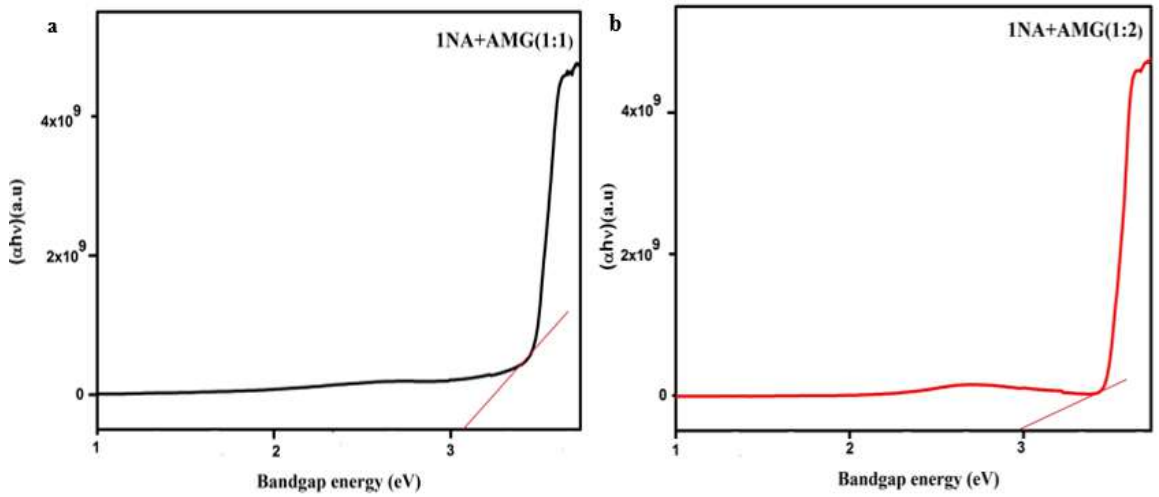

Figure 4.4 *Band gap energy of a) [$(CH_5N_4)\{(C_{10}H_7)(1\text{-}COO)\}$] b) [$(CH_5N_4)_2\{(C_{10}H_7)(1\text{-}COO)\}$]*

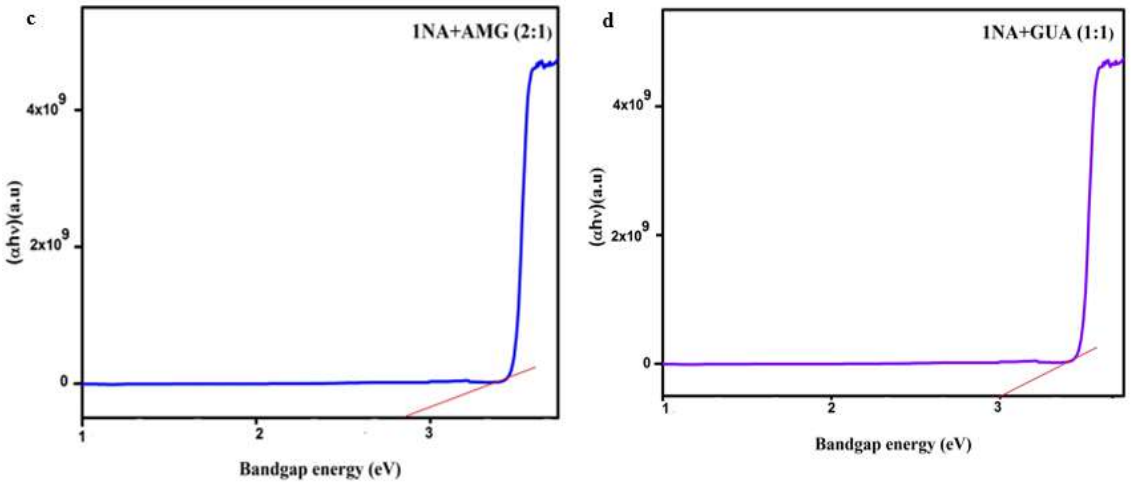

Figure 4.4 *Band gap energy of c) [(CH_5N_4){($C_{10}H_7$)(1-COO)}$_2$] d) [(CH_4N_3){($C_{10}H_7$)(1-COO)}]*

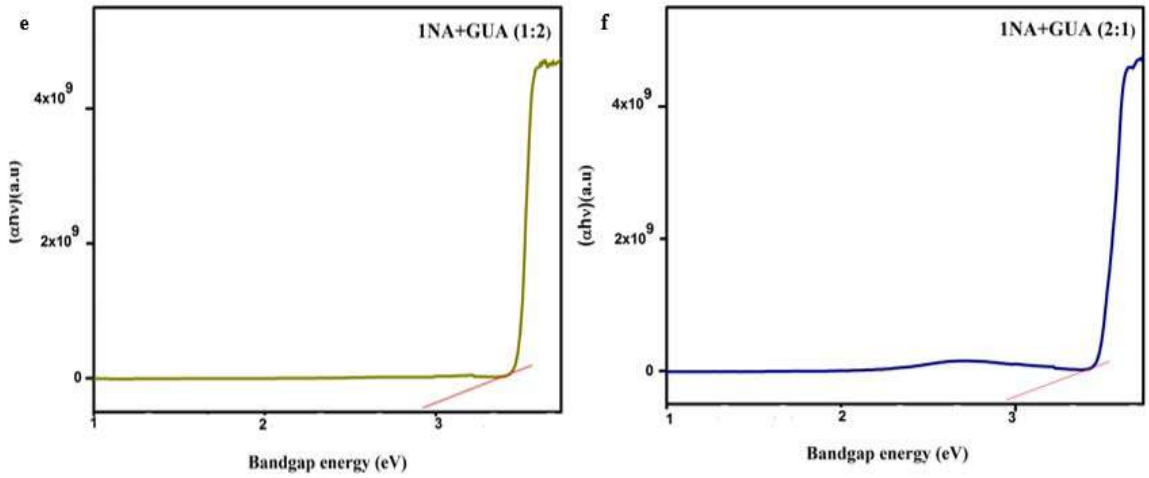

Figure 4.4 *Band gap energy of e) [(CH_4N_3)$_2$){($C_{10}H_7$)(1-COO)}] f) [(CH_4N_3){($C_{10}H_7$)(1-COO)}$_2$]*

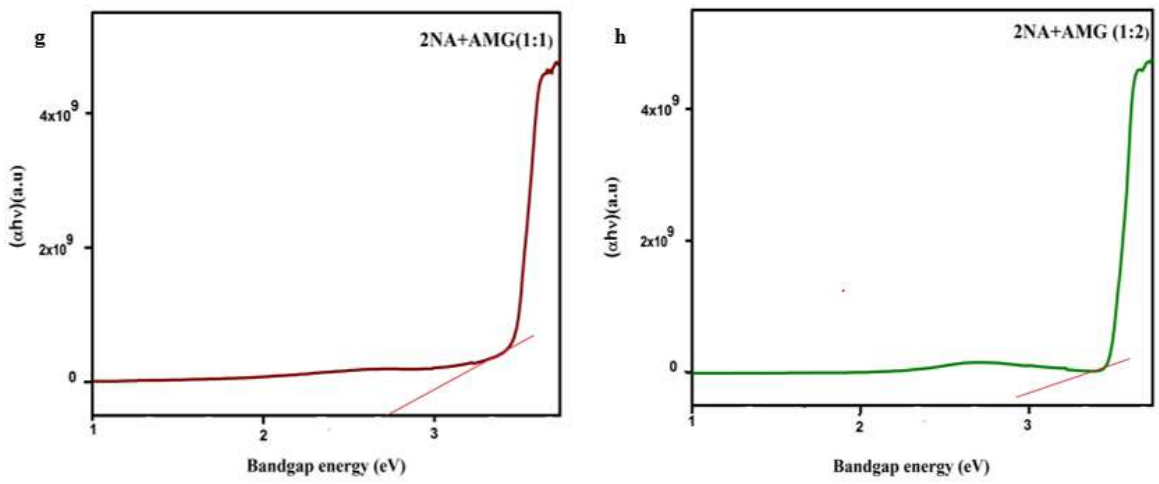

Figure 4.4 *Band gap energy of g) [(CH_5N_4){($C_{10}H_7$)(2-COO)}] h) [(CH_5N_4)$_2${($C_{10}H_7$)(2-COO)}]*

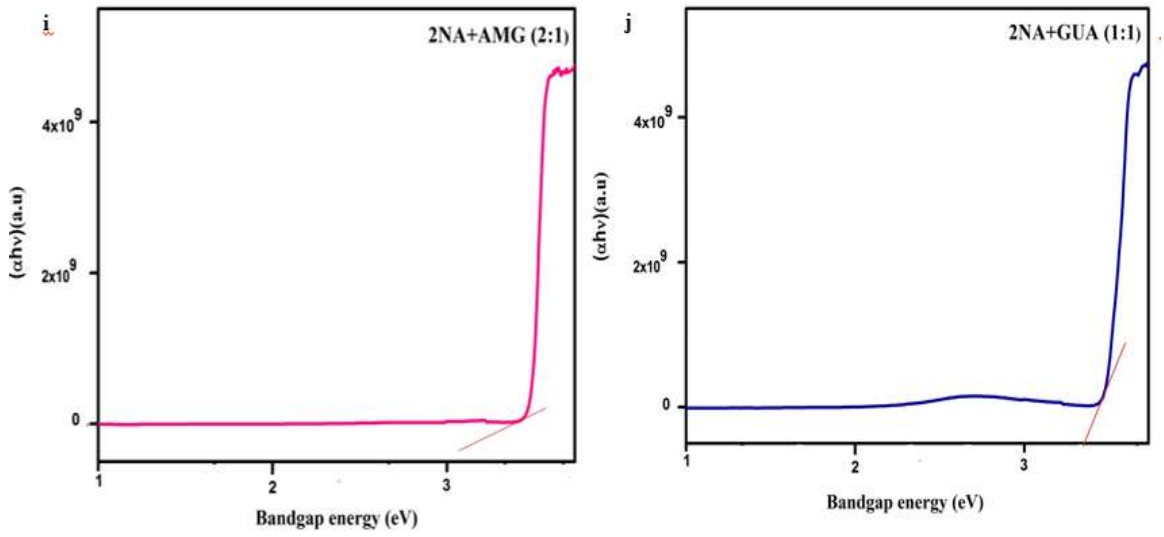

Figure 4.4 *Band gap energy of i) [(CH_5N_4){($C_{10}H_7$)(2-COO)}$_2$] j) [(CH_4N_3){($C_{10}H_7$)(2-COO)}]*

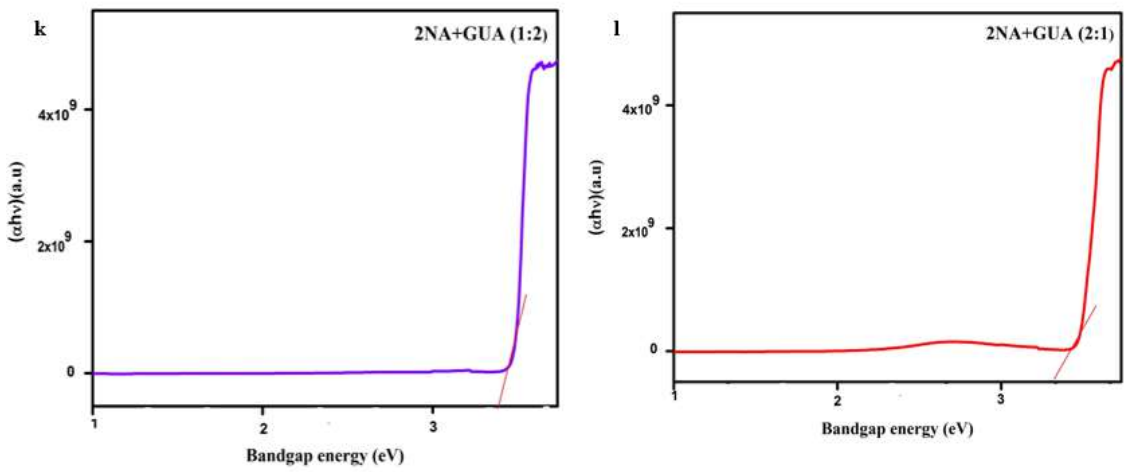

Figure 4.4 *Band gap energy of k) [$(CH_4N_3)_2\{(C_{10}H_7)(2\text{-}COO)\}$]l) [$(CH_4N_3)\{(C_{10}H_7)(2\text{-}COO)\}_2$]*

4.3.4 Thermal analysis

4.3.4.1 Salt of 1-naphthoic acid with aminoguanidine

The salt exhibits a continuous mass loss up to 380 °C and is stable up to 287 °C. As a result, the entire salt is broken down in a single step, as shown in (**Figure 4.5 (a)**). A large endothermic peak at 147 °C and an exothermic peak at 276 °C in DTA. A minor weight loss step from 297 °C to 396 °C is represented by the second peak on the DTA curve, which is located at 367 °C. Carbon residue is left as a final result at 446 ºC.

Figure 4.5 (b), a slight weight loss between 40 °C and 105 °C can be attributed to the dehydration of acid moiety which is confirmed by the presence of an endothermic peak in the DTA. The major weight loss that happens between 105 and 460 °C is due to the removal of the hydroxyl group and other unstable components existing in the sample. Though, beyond 460 °C, there is only a slow weight loss in the sample, which may result in formation residues [8].

From the figure **Figure 4.5 (c)**, it is evident that there are distinct regions of endotherms. These endotherms are in the range of 104,245,281 º C and the exothermic peak occurred at 219 and 258 º C without changing mass loss there is a formation of adduct. Beyond, 438 º C there was no residue was obtained.

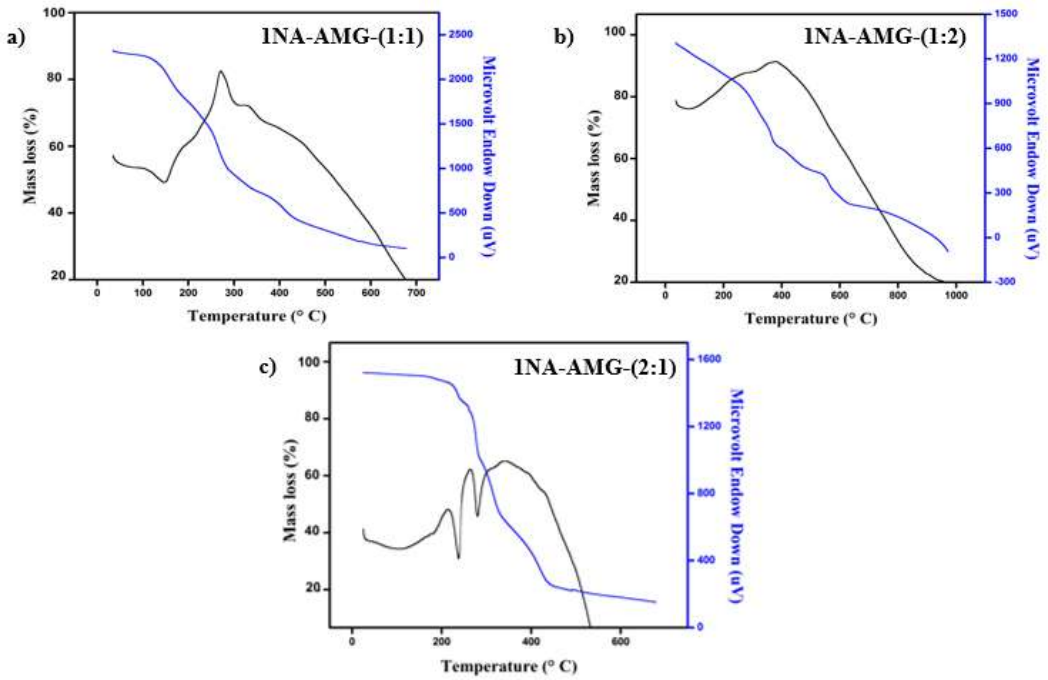

Figure 4.5 *TG-DTA curve of*

a) *$[(CH_5N_4)\{(C_{10}H_7)(1\text{-}COO)\}]$*

b) *$[(CH_5N_4)_2\{(C_{10}H_7)(1\text{-}COO)\}]$*

c) *$[(CH_5N_4)\{(C_{10}H_7)(1\text{-}COO)\}_2]$*

4.3.4.2 Salt of 1-naphthoic acid with guanidine

Figure 4.6 (a), it can be seen that the thermal decomposition process due to dehydration, exhibits endothermic peak at 93, 142, and 309 °C. These peaks are due to loss of moisture content and phase change. Finally, complete decomposition of the salt occurs at 323°C [9].

The salt in the ratio 1:2 melts at 77 °C with no weight loss in TG (**Figure 4.6 (b)**). Further heating, decomposes the organic moiety present in guanidine at 148 °C and shows exotherm in the thermogram. The intermediate is found to be unstable and the final decomposition occurred at 437 °C.

Figure 4.6 (c) illustrates single-phase decomposition by strong exothermic peak around 286 °C is related toward the decomposition of organic moieties. When the temperature was increased from 405 to 600 °C, there is a formation of carbon as a final residue [10].

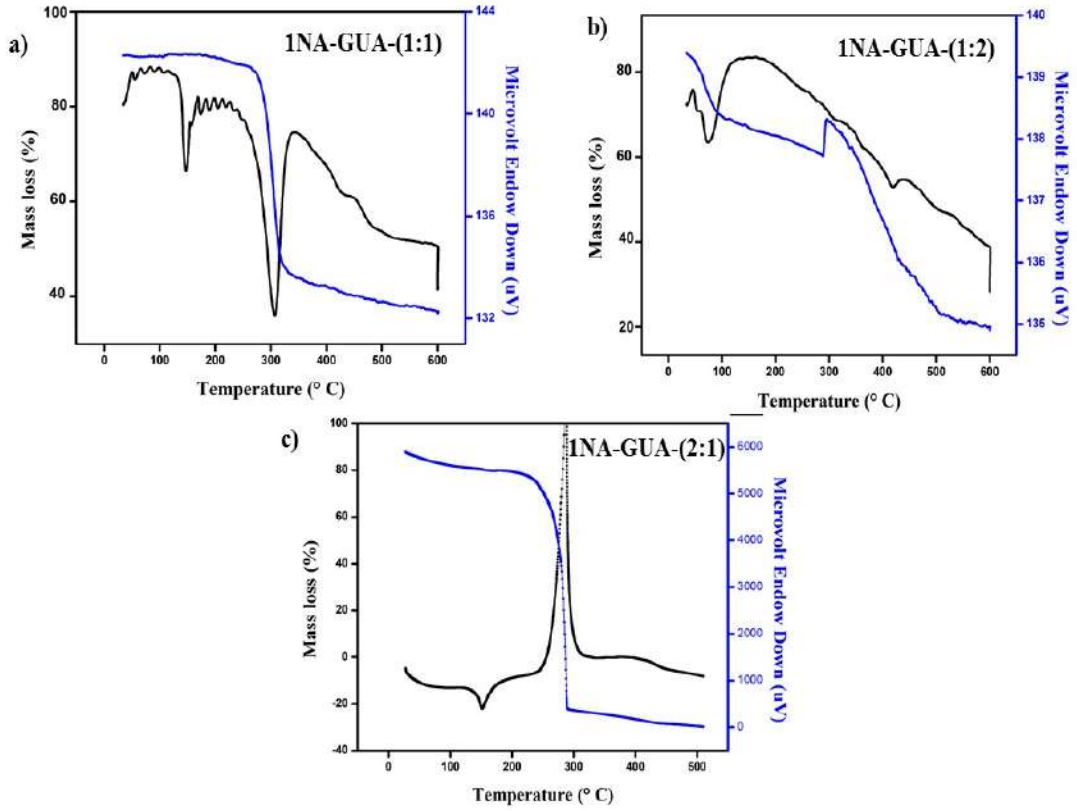

Figure 4.6 *TG-DTA curve of*

a) [(CH4N3){(C10H7)(1-COO)}]

b) [(CH4N3)2{(C10H7)(1-COO)}]

c) [(CH4N3){(C10H7)(1-COO)}2]

4.3.4.3 Salt of 2-naphthoic acid with aminoguanidine

The TGA curve analysis (**Figure 4.7 (a)**) exposed an initial weight loss temperature occurring from 30 °C to 100 °C, due to the removal of volatile compounds. Additionally, the material undergoes a major mass loss between 148 °C to 312 °C indicating the decomposition of the material. From the thermal analysis, we determined the compound is stable up to 319 °C [11].

Figure 4.7 (b,c) revealed a weight loss from 37 °C to 100 °C, is due to removal of physically adsorbed compound. Further, the material undergoes major mass loss between 267 °C to 328 °C indicating the decomposition of the aminoguanidine moiety [12].

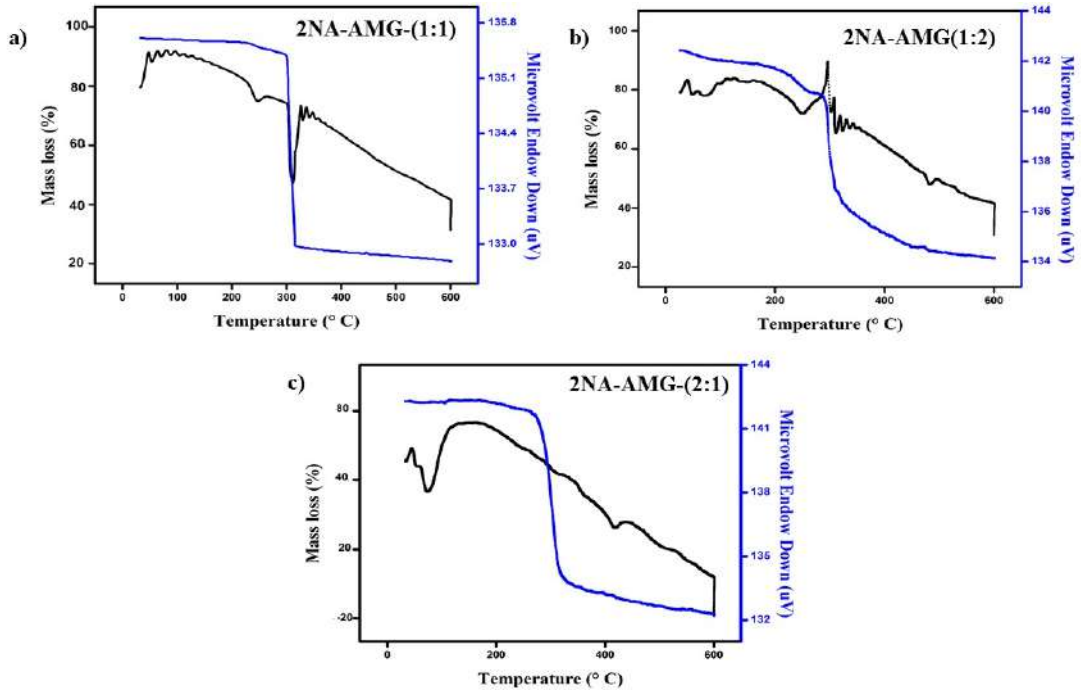

Figure 4.7 *TG-DTA curve of*

a) *$[(CH_5N_4)\{(C_{10}H_7)(2\text{-}COO)\}]$*

b) *$[(CH_5N_4)_2\{(C_{10}H_7)(2\text{-}COO)\}]$*

c) *$[(CH_5N_4)\{(C_{10}H_7)(2\text{-}COO)\}_2]$*

4.3.4.4 Salt of 2-naphthoic acid with guanidine

Both the salts, shown in **Figure 4.8 (a & b)** displays sharp endothermic peak around 270 – 297 °C which is encompassed with many secondary peaks due to the removal of less sable compounds.The acid sdducts was thermally withstand upto 474 °C and finally leads to the formation of carbon residue.

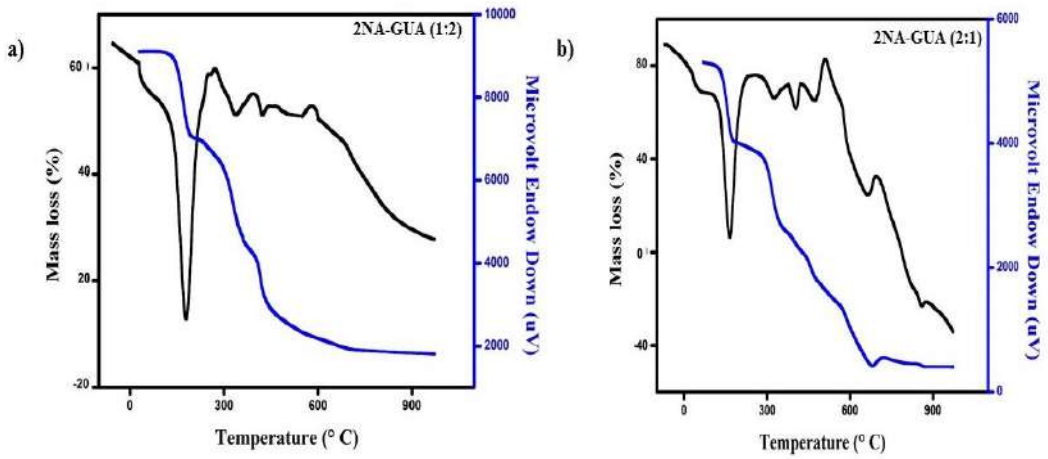

Figure 4.8 *TG-DTA curve of*

a) [$(CH_4N_3)_2${$(C_{10}H_7)$(1-COO)}]

b) [(CH_4N_3){$(C_{10}H_7)$(1-COO)}$_2$]

4.4 CONCLUSION

1- naphthoic acid, and 2-naphthoic acid show similarity in the formation of salt with aminoguanidine/ guanidine. The stabilization of acid adducts is facilitated by hydrogen bonds, which include intermolecular bonds between OH, COOH, $CH_5N_4^{+,}$ and $CH_4N_3^+$ for the crystal intra-molecular bonding found with guanidine. The presence of FT-IR peaks around υNH,υN-N, and υC-N evidence for the formation of salts. The bandgap energy for all the ligands exhibits a range of 2.5-3.5 eV. The TG-DTA for 1- naphthoic acid/2-naphthoic acid confirms their thermal stability.

Table 4.4 *Thermal Analysis*

Metal complexes	DTA peak	Thermogravimetry			Decomposition Nature of the compound
		Temp Range(°C)	Weight loss (%)		
			Obsd.	Calcd.	
$[(CH_5N_4)\{(C_{10}H_7)(1\text{-}COO)\}]$	147(+)	95-231	90	89	Dehydration and partial decomposition
	274(-)	256-700	98.9	-	Complete decompose
$[(CH_5N_4)_2\{(C_{10}H_7)(1\text{-}COO)\}]$	97(+)	40-152	90	90	Decomposition of the organic moiety
	366(-)	301-461	100	100	Completely decomposition
$[(CH_5N_4)\ \{(C_{10}H_7)(1\text{-}COO)\}_2]$	233(+), 274(+)	174-321	79	-	Decomposition of the organic moiety
	326(-)	315-401	100	100	Completely decomposition
$[(CH_4N_3)\{(C_{10}H_7)(1\text{-}COO)\}]$	146(+), 309(+)	100-320	90	90	Dehydration and partial decomposition
	342(-)	320-700	100	100	Complete formation of carbon residue
$[(CH_4N_3)_2\{(C_{10}H_7)(1\text{-}COO)\}]$	73(+)	100-160	97.9	-	Partial decomposition
	443(-)	350-700	100	100	Carbon as final residues
$[(CH_4N_3)\ \{(C_{10}H_7)(1\text{-}COO)\}_2]$	312(+)	100-350	97.9	-	Partial decomposition
	340(-)	350-700	100	100	Carbon as final residues

Metal complexes	DTA peak	Thermogravimetry			Decomposition Nature of the compound
		Temp Range(°C)	Weight loss (%)		
			Obsd.	Calcd.	
$[(CH_5N_4)\{(C_{10}H_7)(2\text{-}COO)\}]$	247(+)	100-260	80	-	Decomposition of the organic moiety
	293(-)	272-700	100	100	Complete decomposition
$[(CH_5N_4)_2\{(C_{10}H_7)(2\text{-}COO)\}]$	75(+)	100-160	80	-	Decomposition of the organic moiety
	449(-)	358-700	100	100	Complete decomposition
$[(CH_5N_4)\ \{(C_{10}H_7)(2\text{-}COO)\}_2]$	278(+)	119-250	80	-	Melting to the decomposition
	557(-)	250-700	100	100	Completely decomposition
$[(CH_4N_3)_2\{(C_{10}H_7)(2\text{-}COO)\}]$	172(+)	162-229	14.9	14.9	Decomposition of ligand group
	519(-)	335-700	100	100	Completely decomposition
$[(CH_4N_3)\ \{(C_{10}H_7)(2\text{-}COO)\}_2]$	147(-)	100-160	80	-	Removal ligand group
	284(+)	250-354	100	100	Fully decomposition

Endothermic = (+), Exothermic = (-)

REFERENCES

1. Arunadevi, N. *et al.* Structural, optical, thermal, biological and molecular docking studies of guanidine based naphthoate metal complexes. *Surfaces and Interfaces* **24**, 101094 (2021).
2. Arunadevi, N. & Vairam, S. 3-hydroxy-2-naphthoate complexes of transition metals with hydrazine-preparation, spectroscopic and thermal studies. *E-Journal Chem.* **6**, (2009).
3. Swathika, M. *et al.* Design and synergistic effect of nano-sized epoxy-NiCo2O4 nanocomposites for anticorrosion applications. *RSC Adv.* **12**, 14888–14901 (2022).
4. Drozd, M. & Dudzic, D. The guanidine and benzoic acid (1:1) complex. The polarized vibrational studies and theoretical investigations. *Spectrochim. Acta Part*
5. Arunadevi, N. *et al.* New epoxy-Nano metal oxide-based coatings for enhanced corrosion protection. *J. Mol. Struct.* **1250**, (2022).
6. Arunadevi, N., Devipriya, S. & Vairam, S. The acid adducts hydrazinium 2-hy-droxy-benzoate-2-hy-droxy-benzoic acid (1/1) and hydrazinium 3-hy-droxy-2-naphtho-ate-3-hy-droxy-2-naphthoic acid (1/1). *Acta Crystallogr. Sect. C Cryst. Struct. Commun.* **68**, o61–o64 (2012).
7. Swathika, M. & Natarajan, A. Synthesis and photometric properties of efficient white-emitting phosphor of M-AMG transition metal complexes for OLED applications. *Luminescence* (2022).
8. Sheikh, R. A., Wani, M. Y., Shreaz, S. & Hashmi, A. A. Synthesis, characterization and biological screening of some Schiff base macrocyclic ligand based transition metal complexes as antifungal agents. *Arab. J. Chem.* **9**, S743–S751 (2016).
9. Tan, Y. X. *et al.* Syntheses, Crystal Structures an Benzyltin Complexes Based on 2-nd Biological Activity of the 1D ChaiOxo-Propionic Acid Benzoyl Hydrazone.
10. Li, Y. *et al.* 3D hierarchical porous nitrogen-doped carbon/Ni@NiO nanocomposites self-templated by cross-linked polyacrylamide gel for high performance supercapacitor electrode. *J. Colloid Interface Sci.* **570**, 286–299 (2020).

11. Poojith, N. *et al.* Y-shaped potential third-order nonlinear optical material-3-(2-amino-2-oxoethyl)-5-methyl hexanoic acid: An analysis of structural, spectroscopic and docking studies. *New J. Chem.* **44**, 18185–18198 (2020).

12. Hussain, S. *et al.* Synthesis, thermal, structural analyses and photoluminescent properties of a new family of malonate-containing Lanthanide(III) coordination polymers. *Front. Chem.* **7**, 1–16 (2019).